

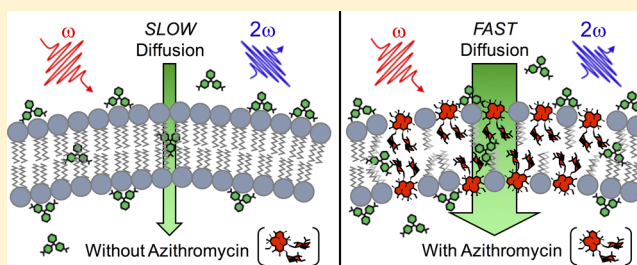
Azithromycin-Induced Changes to Bacterial Membrane Properties Monitored *in Vitro* by Second-Harmonic Light ScatteringMohammad Sharifian Gh.,^{‡,§} Michael J. Wilhelm,^{*,‡,§} and Hai-Lung Dai

Department of Chemistry, Temple University, 1901 North 13th Street, Philadelphia, Pennsylvania 19122, United States

Supporting Information

ABSTRACT: We present a nonlinear light scattering method for monitoring, with real-time resolution and membrane specificity, changes in molecular adsorption, and transport at bacterial membranes induced by an antimicrobial compound. Specifically, time-resolved second-harmonic light scattering (SHS) is used to quantify azithromycin-induced changes to bacterial membrane permeability in colloidal suspensions of living *Escherichia coli*. Variations in membrane properties are monitored through changes in the adsorption and transport rates of malachite green, a hydrophobic cation that gives SHS signal. Regardless of concentration, instantaneous treatment with azithromycin showed no significant changes in membrane permeability. However, 1 h pretreatment with subminimum inhibitory concentrations of azithromycin induced an order-of-magnitude enhancement in the permeability of both the outer membrane and, through facilitation of a new transport mechanism, the cytoplasmic membrane of the bacteria as well. This study illustrates SHS as a novel tool for monitoring antimicrobial-induced changes to membrane properties in living bacteria.

KEYWORDS: Antibiotics, membrane permeability, second-harmonic generation, azithromycin

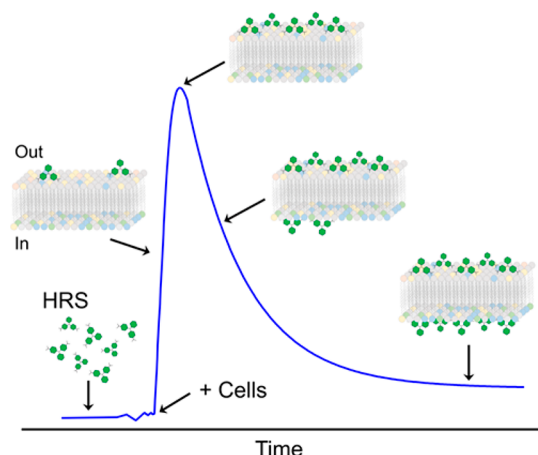


Antimicrobial resistance is a ubiquitous and ongoing problem that diminishes the effectiveness of even the most efficient bactericidal compounds.¹ This worldwide threat demands continued development of new and increasingly innovative pharmaceutical drugs capable of selectively targeting microbial pathogens. To be effective, antimicrobial compounds require the ability to either cross or increase the permeability of the bacteria membrane. In the interest of efficiently optimizing viable antimicrobial targets, it is desirable to develop methodologies capable of monitoring changes to membrane properties in living bacteria.

We have previously demonstrated the utility of second-harmonic light scattering (SHS) for measuring the adsorption and transport rates of molecules at the membranes of living cells.^{2–7} This real-time and surface-sensitive technique has been used for monitoring chemically induced changes to membrane permeability in living cells.⁵ SHS is based on the nonlinear optical phenomenon, second-harmonic generation (SHG), in which a fraction of an incident light of frequency ω is scattered at 2ω after interacting with SHG-active matter.

The fundamental principles of SHS have already been described.^{8–10} SHS is applicable to molecules that exhibit second-order nonlinear polarizability, hereafter denoted as SHG-active, which include molecules lacking inversion symmetry. Scheme 1 depicts the basic mechanism by which SHS can be used to monitor molecular transport across a membrane. When SHG-active molecules are randomly oriented in solution, no coherent SHS is produced due to destructive interference between second harmonic light emitted from

Scheme 1. Characteristic Time-Resolved SHS Signal Response for Molecular Adsorption at the Surfaces of, and Transport Across, a Phospholipid Membrane



neighboring molecules. In this case, only incoherent hyper-Rayleigh scattering (HRS) is produced.^{9,10} However, when such molecules adsorb onto the outer surface of a cell

Special Issue: Med Chem Tech: Driving Drug Development

Received: December 1, 2017

Accepted: March 9, 2018

Published: March 9, 2018

membrane, they align with one another due to similar molecule–membrane interactions. The second harmonic light emitted from these molecules constructively interferes and produces SHS signal. As some of those molecules diffuse across the bilayer and adsorb onto the interior surface of the membrane, SHS from the oppositely oriented molecules on the inner surface cancels with the signal from the molecules remaining on the outer surface. This results in a decrease of the measured SHS. Consequently, the rise in SHS signal is proportional to the rate of molecular adsorption onto the outer surface of the membrane, and the subsequent decay is proportional to the molecular transport rate across the membrane. This interpretation has been extensively validated following numerous studies in which SHS has been used to study molecular adsorption and transport across membranes in biomimetic liposomes^{11–16} and living cells.^{2–7}

In this letter, we show that antibiotic-induced changes to membrane permeability can be quantitatively discerned through real-time monitoring of the transport rate of an SHG-active probe molecule. Specifically, the transport of the probe molecule is first characterized in a sample containing healthy viable bacteria. The experiment is then repeated, but with the addition of an antibiotic, within proximity of the minimum inhibitory concentration (MIC), and for a variety of incubation times, to induce changes in the properties of the bacterial membrane(s). For instance, an increase in membrane permeability allows transport of the SHG-active probe to occur at a faster rate, which can be quantitatively verified through analysis of the time-dependent SHS measurement.

Macrolides form a general class of antibiotic compounds whose structure contains a large macrocyclic lactone ring. As a group, they have been effectively used in clinical treatments, primarily against Gram-positive based infections, for well over 50 years.¹⁷ The proposed mechanism-of-action is rooted in the inhibition of bacterial protein synthesis due to binding of the macrolide to the 50S ribosomal subunit of the bacterial 70S ribosomes.¹⁷ Azithromycin (AZM) is one of the more recently developed macrolides with improved antimicrobial effectiveness that extends even to Gram-negative species due to the addition of a methyl-substituted nitrogen in the azalide ring.^{18–20} Given the bulky nature of macrolides, as well as the fact that they must travel to the cytoplasm before they can induce an antimicrobial effect, there has been considerable interest in characterizing macrolide–membrane interactions.

For instance, AZM has a molecular weight of 749 Da, well over the exclusion limit (~600 Da) for passive diffusion across the outer membrane protein (Omp) porin channels located in the outer membrane (OM) of Gram-negative bacteria.^{18–20} Nevertheless, it has been suggested that AZM can rapidly traverse the OM through the so-called “self-promotion uptake route” by disrupting the lipopolysaccharide (LPS) chains, resulting in enhanced permeability of the *outer leaflet* of the OM.^{18–20} Several studies have examined the interaction of AZM with biomimetic membrane systems^{21–24} and provided insight into how AZM may interact with a bacterial cytoplasmic membrane (CM). The current consensus is that macrolides alter phospholipid organization and membrane fluidity.^{21–24}

We report here the application of time-resolved SHS to quantitatively monitor the concentration- and time-dependent interactions of AZM with the two phospholipid membranes of the Gram-negative bacteria, *Escherichia coli* (*E. coli*). Specifically, we measure the time-dependent uptake of the SHG-active cation, malachite green (MG), in colloidal suspensions of living

E. coli that have been treated with increasing concentrations of AZM for durations of either 0 or 1 h. Quantitative analysis of the time-resolved SHS signals reveals AZM-induced changes to bacterial membrane permeability.

We first demonstrate that our strain of *E. coli* is susceptible to the antibiotic effects of AZM. The MIC was deduced using the broth dilution method²⁵ and quantified with flow cytometry (see Supporting Information, SI, for additional details). It must be noted, however, that our SHS experiments require higher cell densities to yield measurable signal. Consequently, a MIC assessment was also performed for higher cell density. In general, as cell density increases, the MIC also increases.²⁵ As expected, for the elevated cell density, the MIC increased from 0.5 to 128 $\mu\text{g}/\text{mL}$ (see SI). Nevertheless, for both high and low cell densities, the ratio of the MIC to the cell density was roughly equal, ca. 10^9 molecules per cell, suggesting that the same mechanism is at play for both conditions.

Details of our SHS experiment can be found in the SI. Briefly, the 800 nm output from a femtosecond Ti:sapphire oscillator was focused into the center of a continuously flowing liquid jet containing a solution of 25 μM MG and variable concentrations of AZM. Light scattered at the second harmonic of the laser (400 nm) was collected in the forward propagation direction. At $t = 0$, a colloidal suspension of living *E. coli* (in phosphate buffered saline) was added to the liquid reservoir. Adsorption of MG onto the bacterial membrane surfaces results in production of a time-dependent SHS signal.

Figure 1 shows representative time-resolved SHS traces recorded after living *E. coli* was added to solutions containing

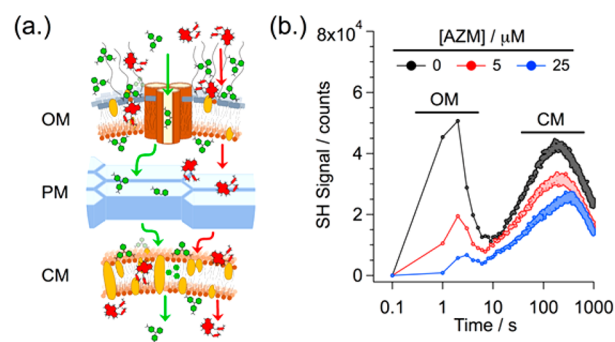


Figure 1. (a) Cartoon schematic of adsorption/transport of MG (green) and AZM (red) with respect to the ultrastructure of Gram-negative bacteria. (b) Time-resolved SHS signal, plotted in log time, monitoring uptake of MG by *E. coli* in increasing concentrations of AZM. SHS intensities are in units of photon counts.

25 μM MG and increasing concentrations of AZM. At high concentrations, MG can act as an antibiotic. Hence, the static MG concentration was set to be well below the MIC (100 μM , see SI) but sufficiently high to provide strong signal at increased AZM concentrations. A schematic of molecular uptake in Gram-negative bacteria is shown to illustrate the process that SHS is monitoring. The ultrastructure of Gram-negative bacteria consists of dual phospholipid membranes (Figure 1a): an OM coated with anionic LPS and perforated with water-filled Omp channels that permit passive diffusion of small molecules, and an inner CM. The two membranes are separated by a thin peptidoglycan mesh (PM) that acts as a diffusion barrier. Due to the presence of the two membranes, the time-resolved SHS signal exhibits two distinct sequential transport events (Figure 1b, black trace). Note that time has

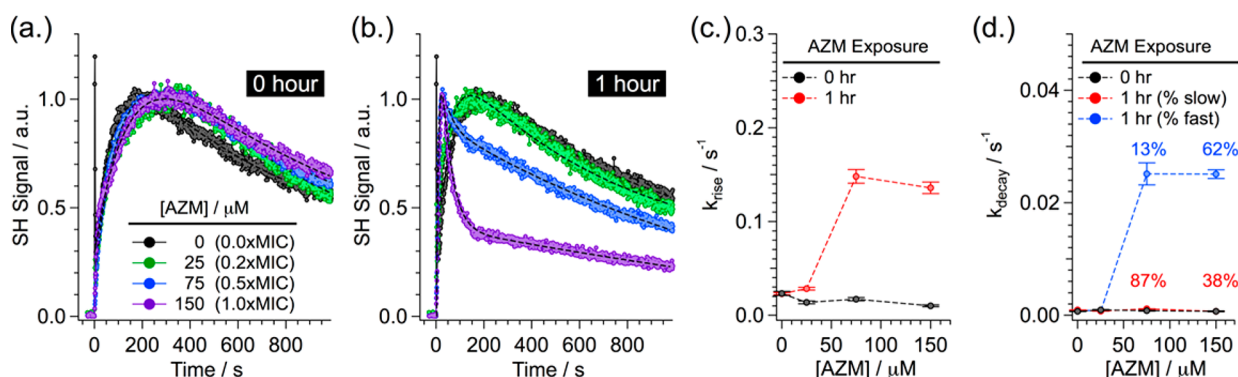


Figure 2. Representative time-resolved SHS signal collected during bacterial uptake of MG following (a) 0 h or (b) 1 h exposure to 0 (black), 25 (green), 75 (blue), or 150 μM (purple) AZM. SHS intensities have been normalized to the CM transport peak. Dashed lines represent best fit results. Fit deduced rate constants corresponding to (c) adsorption onto the outer surface of the CM and (d) transport across the CM, as a function of AZM concentration. The relative fraction of fast (blue) and slow (red) transport are annotated above the corresponding markers in (d). Error bars depict standard deviation of the rates from minimally $n = 3$ trials for each AZM concentration.

been plotted on a logarithmic scale to simultaneously display both fast and slow events. The initial fast event, with a rise and decay spanning 0.1 to 10 s, is assignable to MG adsorption onto the outer surface of the OM, and then rapid transport across the OM. This is followed by a much slower secondary transport event spanning 10 to >1000 s. The slow second rise near 10 s stems from hindered diffusion of MG across the PM and subsequent adsorption onto the outer surface of the CM. Likewise, the slow second decay starting at ~ 200 s stems from transport of MG across the CM and adsorption onto the interior surface of the CM.

MG and AZM are both cationic and compete for anionic surface adsorption sites. As the concentration of AZM increases, less MG is able to adsorb onto the membrane surface. Under the current experimental conditions, AZM does not produce a measurable SHS signal. As a result, competitive adsorption of AZM onto the membrane results in a reduction in the total SHS signal measured. Specifically, compared to the 0 μM AZM case (Figure 1b, black trace), addition of 5 μM AZM results in a 60% reduction in the measured SHS signal from the OM (Figure 1b, red trace). As the AZM concentration continues to increase, less signal is observed at the OM. For equivalent concentrations of MG and AZM (25 μM , $0.2 \times$ MIC), the OM signal effectively disappears (90% reduction, Figure 1b, blue trace). This suggests that AZM, which is polycationic (+2 charge), successfully competes against cationic MG (+1 charge) for anionic surface adsorption sites. Notice that a less-pronounced competition-induced reduction of SHS is also observed for the CM ($\sim 30\%$ reduction for 5 μM AZM, Figure 1b). Consequently, despite the fact that AZM is too large to traverse the Omp channels,^{18–20} our results strongly suggest that it is still able to rapidly cross the OM (and PM) and arrives at the CM with a rate similar to MG.

Figure 2 highlights the effects of increasing concentrations of AZM (0 to 150 μM , 0 to $1 \times$ MIC) on bacterial membrane properties. AZM was exposed to the cells for either 0 (Figure 2a) or 1 h (Figure 2b) prior to initiating the SHS experiments. For all measurements, the concentration of MG was maintained at 25 μM . As discussed above, for high AZM concentrations, we no longer observe the OM SHS transport peak due to competitive or hindered adsorption of MG in the presence of AZM (Figure 2b). Note, this is not evidence of an AZM-induced enhancement in OM permeability. Rather, competition for surface adsorption sites reduces the adsorption rate of MG.

Under these conditions, MG crosses the OM before it has a chance to adsorb onto the outer surface of the OM, and hence, no SHS signal is produced. In contrast, we still observe the SHS transport event at the CM. This is because the MG transport rate across the CM is orders of magnitude slower (compared to the OM), and so saturation of the CM surfaces still occurs sequentially in time (i.e., outer surface first, then inner surface following transport). Given the complete loss of the OM transport event for high AZM concentrations, all information regarding AZM-induced variations in either the OM or CM properties must therefore be inferred from changes to the measured MG adsorption and transport rates at the CM.

For the instantaneous exposure cases (Figure 2a, AZM added at $t = 0$), the adsorption (signal rise) and transport (signal decay) rates of MG at the CM are nearly identical for all AZM concentrations. For ease of comparison, the measured SHS signals have been normalized to the CM transport peak. Variations in the magnitude of the SHS signals may stem from a variety of sources, including changes in cell density and size, as well as orientation of the adsorbed MG (see SI),²⁶ which may change in response to surface crowding effects of coadsorbed AZM. While these effects change the magnitude of the SHS signal, they do not alter the kinetics.

The invariance of the observed kinetics in the instantaneous exposure cases suggests that while both AZM and MG are present at the CM following transport across the OM and PM, AZM has not yet had sufficient time to alter the membrane properties. In contrast, for the 1 h exposure cases (Figure 2b), higher concentrations of AZM induced significant variations in the membrane permeability of both the OM and CM. Specifically, for 25 μM AZM ($0.2 \times$ MIC, green trace), there is no significant change in the adsorption or transport properties. However, for 75 μM ($0.5 \times$ MIC, blue trace) and 150 μM AZM ($1 \times$ MIC, purple trace), the rate of MG adsorption onto the outer surface of the CM, and the transport rate across the CM have increased substantially.

As shown in Figure 2a,b, for instantaneous exposure or low AZM concentrations ($\leq 25 \mu M$, $0.2 \times$ MIC), the CM transport event is well described by a single slow exponential decay. However, for higher AZM concentrations ($\geq 0.5 \times$ MIC) over longer durations, the CM transport event clearly consists of at least two decay processes. In order to quantitatively analyze the AZM-induced changes to membrane properties, the measured SHS signals in Figure 2 were fit to a phenomenological model,

consisting of a sequential exponential rise and multiple decays of signal. The key observable for the current study is the relative change of the transport rate of the CM. Under the condition that the OM transport rate is orders of magnitude faster than that of the CM, the later can be deduced as the exponential decay of the SHS signal. Specifically, the time-dependent SHS signal, which is proportional to the square of the MG surface density,^{8–10} was modeled as

$$\sqrt{\text{SHS}(t)} = \varphi_0 + \varphi_1 [1 - \exp(-k_{\text{rise}}t)] [\chi_{\text{fast}} \exp(-k_{\text{decay}}^{\text{fast}}t) + \chi_{\text{slow}} \exp(-k_{\text{decay}}^{\text{slow}}t)] \quad (1)$$

where φ_0 is a baseline offset; φ_1 is an intensity scaling factor; k_{rise} , $k_{\text{decay}}^{\text{fast}}$, and $k_{\text{decay}}^{\text{slow}}$ are rate constants for surface adsorption and fast and slow membrane transport, respectively; and χ_{fast} and χ_{slow} are proportionality constants describing the relative fraction of fast and slow transport across the CM.

The MG adsorption and transport rate constants at the CM for increasing concentrations of AZM, obtained from nonlinear least-squares fits using eq 1, are summarized in Figure 2c,d. For low AZM concentrations ($\leq 25 \mu\text{M}$, $0.2 \times \text{MIC}$) and instantaneous exposure, there is no variation in the adsorption (Figure 2c, black markers) or transport rates (Figure 2d, black markers). However, for higher AZM concentrations ($> 25 \mu\text{M}$) and longer exposure times, the CM surface adsorption rates increase by an order of magnitude. This suggests an increase in the permeability of the OM (i.e., a higher concentration of MG is now able to cross the OM and arrive at the outer surface of the CM). Further, the dual decay behavior observed in Figure 2b for CM transport events following 1 h exposure to either $75 \mu\text{M}$ ($0.5 \times \text{MIC}$) or $150 \mu\text{M}$ ($1 \times \text{MIC}$) AZM were fit to determine the rate constants of the fast and slow transport processes. The rate of the slow transport process (Figure 2d, red markers) was shown to be effectively identical to the unperturbed rates (black markers). Conversely, the fast transport process (blue markers) exhibited significantly enhanced rates. Further, the relative efficiency of the fast transport process (χ_{fast}) was observed to increase with AZM concentration. Overall, the fast decay process was not observed in the $25 \mu\text{M}$ ($0.2 \times \text{MIC}$) AZM case, but it accounted for 13% of the $75 \mu\text{M}$ ($0.5 \times \text{MIC}$) AZM case and increased to 62% for $150 \mu\text{M}$ ($1 \times \text{MIC}$) AZM. This suggests that accumulation of increasing concentrations of AZM creates an efficient secondary transport route across the CM.

All prior studies examining AZM–membrane interactions can be categorized into one of two groups focusing on interactions with either (1) the bacterial OM in living cells^{18–20} or (2) CMs in model membrane systems.^{21–24} The interaction of AZM with the OM of Gram-negative bacteria has been extensively studied using a time-resolved fluorescence-based assay employing the chromophore, 1-N-phenyl-naphthyl-amine (NPN).²⁷ Of significance, transitioning from a hydrophilic to a hydrophobic environment increases the fluorescence intensity of NPN four-fold. Experiments in which AZM was added to solutions containing Gram-negative bacteria and NPN showed an immediate increase in fluorescence intensity that could not be repeated in either liposome-based or LPS-compromised systems.^{18–20} This hinted at a rapid interaction between AZM and the bacterial LPS, which allowed for efficient shuttling of NPN into the hydrophobic interior of the OM. The resulting interpretation was that exposure to AZM yields an instantaneous increase in the permeability of the outer leaflet of the OM.

The majority of studies have probed the interaction of AZM with model membrane systems.^{21–24,28,29} For example, ³¹P nuclear magnetic resonance spectroscopy has been used to characterize AZM-induced variations in interactions between nearest neighbor phospholipid head groups.^{21,28,29} In particular, membrane-inserted AZM electrostatically binds to anionic phospholipids.^{21,29} This reduces the mobility of the phospholipid head but increases the fluidity of the hydrophobic acyl chains.²⁹ Similarly, complementary studies using atomic force microscopy revealed AZM-induced variations in the phospholipid organization of the membrane.^{21,22} It has been suggested that AZM inserts itself into the bilayer at the interface between the phospholipid head groups and the fatty acyl chains,²³ thereby disrupting the phospholipid organization.

While all prior studies dealt with either a single component of the complex bacterial membrane system or biomimetic model membranes and provided useful insights on the macrolide–membrane interactions, our approach illustrates the ability to concurrently examine the effects of macrolides on the permeability of all bacterial membranes. Our current results are fully consistent with all prior experimental studies. Specifically, even though AZM is too large to traverse the bacterial Omp channels, time-resolved SHS reveals that AZM is able to rapidly diffuse across the OM. However, even at high concentrations, instantaneous exposure to AZM is not sufficient to induce changes in the permeability of either the OM or CM. It is only after sufficiently high concentrations of AZM are allowed to interact with the cells for a prolonged duration that the membrane properties begin to change. Of significance, our observations reveal that accumulation of AZM, even for sub-MIC conditions, creates an efficient secondary transport route across the CM, the propensity of which increases with AZM concentration. This behavior is reminiscent of the so-called carpet disruption mechanism³⁰ for cell-penetrating peptides. While it is speculative to suggest that AZM is creating well-defined pores across the membrane, it is also feasible to consider that, similar to the proposed carpet disruption mechanism,³⁰ AZM induces localized thinning of the membrane. The density of such regions would scale with AZM concentration and would allow for comparatively rapid transport across the membrane. We present these speculations with the hope that our observations will inspire other experimental or computational studies to further investigate this phenomenon.

In summary, we have demonstrated that time-resolved SHS, with MG as an SHG-active probe, can be used to quantify the concentration- and time-dependent interactions of AZM with the dual membranes of living *E. coli*. The fact that MG passively transports across bacterial membranes (even in the absence of antibiotic attack) means it is an excellent reporter of membrane properties. In this way, time-resolved SHS (using MG as a probe) is universally applicable for sequentially monitoring antimicrobial-induced changes in individual membranes of living bacteria. It is observed that prolonged treatment with sub-MIC AZM induces a dramatic increase in the rate of transport of the SHG-active probe across both the OM and CM of the bacteria. Our observations suggest that the observed fast transport route through the CM is likely facilitated by the creation of a new mechanism induced by the interaction of AZM with the CM.

■ ASSOCIATED CONTENT

Supporting Information

The Supporting Information is available free of charge on the ACS Publications website at DOI: 10.1021/acsmchemlett.7b00499.

Experimental methods, including sample preparation and details regarding the time-resolved SHS setup (PDF)

■ AUTHOR INFORMATION

Corresponding Author

*E-mail: michael.wilhelm@temple.edu.

ORCID

Mohammad Sharifian Gh.: 0000-0003-3867-1611

Michael J. Wilhelm: 0000-0002-4634-9561

Author Contributions

[‡]These authors contributed equally to this work. M.S.G. and M.J.W. conceived/designed the experiments; M.S.G. performed the experiments; M.S.G. and M.J.W. analyzed the data; M.S.G., M.J.W., and H.L.D. interpreted the results; and M.J.W. wrote the manuscript with input from the other authors.

Funding

This work was supported by the National Science Foundation (Grant CHE-1465096).

Notes

The authors declare no competing financial interest.

■ ABBREVIATIONS

AZM, azithromycin; CM, cytoplasmic membrane; *E. coli*, *Escherichia coli*; LPS, lipopolysaccharide; MG, malachite green; MIC, minimum inhibitory concentration; NPN, 1-N-phenyl-naphthyl-amine; OM, outer membrane; Omp, outer membrane protein; PM, peptidoglycan mesh; SHG, second-harmonic generation; SHS, second-harmonic laser scattering

■ REFERENCES

- (1) WHO. *Antibacterial Agents in Clinical Development: An Analysis of the Antibacterial Clinical Development Pipeline, Including Tuberculosis*; World Health Organization: Geneva, 2017.
- (2) Zeng, J.; Eckenrode, H. M.; Dounce, S. M.; Dai, H.-L. Time-Resolved Molecular Transport across Living Cell Membranes. *Biophys. J.* **2013**, *104*, 139–145.
- (3) Wilhelm, M. J.; Sheffield, J. B.; Gonella, G.; Wu, Y.; Spahr, C.; Zeng, J.; Xu, B.; Dai, H.-L. Real-Time Molecular Uptake and Membrane-Specific Transport in Living Cells by Optical Microscopy and Nonlinear Light Scattering. *Chem. Phys. Lett.* **2014**, *605–606*, 158–163.
- (4) Wilhelm, M. J.; Sheffield, J. B.; Sharifian Gh., M.; Wu, Y.; Spahr, C.; Gonella, G.; Xu, B.; Dai, H.-L. Gram's Stain Does Not Cross the Bacterial Cytoplasmic Membrane. *ACS Chem. Biol.* **2015**, *10*, 1711–1717.
- (5) Wilhelm, M. J.; Sharifian Gh., M.; Dai, H.-L. Chemically Induced Changes to Membrane Permeability in Living Cells Probed by Nonlinear Light Scattering. *Biochemistry* **2015**, *54*, 4427–4430.
- (6) Zeng, J.; Eckenrode, H. M.; Dai, H.-L.; Wilhelm, M. J. Adsorption and Transport of Charged vs. Neutral Hydrophobic Molecules at the Membrane of Murine Erythroleukemia (MEL) Cells. *Colloids Surf., B* **2015**, *127*, 122–129.
- (7) Sharifian Gh., M.; Wilhelm, M. J.; Dai, H.-L. Label-Free Optical Method for Quantifying Molecular Transport Across Cellular Membranes In Vitro. *J. Phys. Chem. Lett.* **2016**, *7*, 3406–3411.
- (8) Eisenthal, K. B. Second Harmonic Spectroscopy of Aqueous Nano- and Microparticle Interfaces. *Chem. Rev.* **2006**, *106*, 1462–1477.
- (9) Gonella, G.; Dai, H.-L. Second Harmonic Light Scattering from the Surface of Colloidal Objects: Theory and Applications. *Langmuir* **2014**, *30*, 2588–2599.
- (10) Roke, S.; Gonella, G. Nonlinear Light Scattering and Spectroscopy of Particles and Droplets in Liquids. *Annu. Rev. Phys. Chem.* **2012**, *63*, 353–378.
- (11) Varshney, G. K.; Kintali, S. R.; Das, K. Effect of Curcumin Addition on the Adsorption and Transport of a Cationic Dye across DPPG-POPG Liposomes Probed by Second Harmonic Spectroscopy. *Langmuir* **2017**, *33*, 8302–8310.
- (12) Tran, R. J.; Sly, K. L.; Conboy, J. C. Applications of Surface Second Harmonic Generation in Biological Sensing. *Annu. Rev. Anal. Chem.* **2017**, *10*, 387–414.
- (13) Srivastava, A.; Eisenthal, K. B. Kinetics of Molecular Transport across a Liposome Bilayer. *Chem. Phys. Lett.* **1998**, *292*, 345–351.
- (14) Liu, J.; Shang, X.; Pompano, R.; Eisenthal, K. Antibiotic Assisted Molecular Ion Transport across a Membrane in Real Time. *Faraday Discuss.* **2005**, *129*, 291–299.
- (15) Kumal, R. R.; Nguyenhuu, H.; Winter, J. E.; McCarley, R. L.; Haber, L. H. Impacts of Salt, Buffer, and Lipid Nature on Molecular Adsorption and Transport in Liposomes As Observed by Second Harmonic Generation. *J. Phys. Chem. C* **2017**, *121*, 15851–15860.
- (16) Kim, J. H.; Kim, M. W. Temperature Effect on the Transport Dynamics of a Small Molecule through a Liposome Bilayer. *Eur. Phys. J. E: Soft Matter Biol. Phys.* **2007**, *23*, 313–317.
- (17) Kanoh, S.; Rubin, B. K. Mechanisms of Action and Clinical Application of Macrolides as Immunomodulatory Medications. *Clin. Microbiol. Rev.* **2010**, *23*, 590–615.
- (18) Farmer, S.; Li, Z.; Hancock, R. E. W. Influence of Outer Membrane Mutations on Susceptibility of *Escherichia coli* to the Dibasic Macrolide Azithromycin. *J. Antimicrob. Chemother.* **1992**, *29*, 27–33.
- (19) Imamura, Y.; Higashiyama, Y.; Tomono, K.; Izumikawa, K.; Yanagihara, K.; Ohno, H.; Miyazaki, Y.; Hirakata, Y.; Mizuta, Y.; Kadota, J.; Iglewski, B. H. Azithromycin Exhibits Bactericidal Effects on *Pseudomonas aeruginosa* through Interaction with the Outer Membrane. *Antimicrob. Agents Chemother.* **2005**, *49*, 1377–1380.
- (20) Hancock, R. E. W.; Farmer, S. W.; Li, Z.; Poole, K. Interaction of Aminoglycosides with the Outer Membranes and Purified Lipopolysaccharide and OmpF Porin of *Escherichia coli*. *Antimicrob. Agents Chemother.* **1991**, *35*, 1309–1314.
- (21) Tyteca, D.; Schanck, A.; Dufrene, Y. F.; Deleu, M.; Courtoy, P. J.; Tulkens, P. M.; Mingeot-Leclercq, M. P. The Macrolide Antibiotic Azithromycin Interacts with Lipids and Affects Membrane Organization and Fluidity: Studies on Langmuir-Blodgett Monolayers, Liposomes and J774 Macrophages. *J. Membr. Biol.* **2003**, *192*, 203–215.
- (22) Berquand, A.; Mingeot-Leclercq, M. P.; Dufrene, Y. F. Real-Time Imaging of Drug-Membrane Interactions by Atomic Force Microscopy. *Biochim. Biophys. Acta, Biomembr.* **2004**, *1664*, 198–205.
- (23) Fa, N.; Lins, L.; Courtoy, P. J.; Dufrene, Y.; Van Der Smissen, P.; Bresseur, R.; Tyteca, D.; Mingeot-Leclercq, M. P. Decrease of Elastic Moduli of DOPC Bilayers Induced by a Macrolide Antibiotic, Azithromycin. *Biochim. Biophys. Acta, Biomembr.* **2007**, *1768*, 1830–1838.
- (24) Fa, N.; Ronkart, S.; Schanck, A.; Deleu, M.; Gaigneaux, A.; Goormaghtigh, E.; Mingeot-Leclercq, M. P. Effect of the Antibiotic Azithromycin on Thermotropic Behavior of DOPC or DPPC Bilayers. *Chem. Phys. Lipids* **2006**, *144*, 108–116.
- (25) Wiegand, I.; Hilpert, K.; Hancock, R. E. W. Agar and Broth Dilution Methods to Determine the Minimal Inhibitory Concentration (MIC) of Antimicrobial Substances. *Nat. Protoc.* **2008**, *3*, 163–175.
- (26) de Beer, A. G. F.; Roke, S. Obtaining Molecular Orientation from Second Harmonic and Sum Frequency Scattering Experiments in Water: Angular Distribution and Polarization Dependence. *J. Chem. Phys.* **2010**, *132*, 234702.
- (27) Loh, B.; Grant, C.; Hancock, R. E. W. Use of the Fluorescent Probe 1-N-Phenyl-naphthylamine to Study the Interactions of

Aminoglycoside Antibiotics with the Outer Membrane of *Pseudomonas Aeruginosa*. *Antimicrob. Agents Chemother.* **1984**, *26*, 546–551.

(28) Kosol, S.; Schrank, E.; Bukvic, M.; Wagner, G. E.; Meyer, N. H.; Go, C.; Rechberger, G. N.; Zangger, K.; Novak, P. Probing the Interactions of Macrolide Antibiotics with Membrane-Mimetics by NMR Spectroscopy. *J. Med. Chem.* **2012**, *55*, 5632–5636.

(29) Montenez, J.-P.; Van Bambeke, F.; Piret, J.; Brasseur, R.; Tulkens, P. M.; Mingeot-Leclercq, M.-P. Interactions of Macrolide Antibiotics (Erythromycin A, Roxithromycin, Erythromyclamine [Dirithromycin], and Azithromycin) with Phospholipids: Computer-Aided Conformational Analysis and Studies on Acellular and Cell Culture Models. *Toxicol. Appl. Pharmacol.* **1999**, *156*, 129–140.

(30) Melo, M. N.; Ferre, R.; Castanho, M. A. R. B. Antimicrobial Peptides: Linking Partition, Activity and High Membrane-Bound Concentrations. *Nat. Rev. Microbiol.* **2009**, *7*, 245–250.